PERGAMON

International Journal of Solids and Structures 37 (2000) 5795–5808

INTERNATIONAL JOURNAL OF SOLIDS and STRUCTURES

www.elsevier.com/locate/ijsolstr

Transient response of a crack in piezoelectric strip subjected to the mechanical and electrical impacts: mode-III problem

Xuyue Wang, Shouwen Yu*

Department of Engineering Mechanics, Tsinghua University, Beijing 100084, People's Republic of China

Received 6 February 1999; in revised form 24 September 1999

Abstract

The linear piezoelectricity theory is applied to investigate the dynamic response of a center-situated crack perpendicular to the edges of the piezoelectric strip subjected to anti-plane mechanical and electrical impacts. Integral transforms and dislocation density functions are employed to reduce the problem to Cauchy singular integral equations. Numerical results show the effects of loading combination and the ratio of crack length to strip width on the dynamic stress intensity factor and the dynamic energy release rate. Two cases of crack surface conditions, impermeable and electrical contact, are considered. For an impermeable crack, the dynamic energy release rate may be used as the crack extension force, whereas for an electrical contact crack, the dynamic stress intensity factor remains the fracture parameter at the crack tip since the electrical field does not contribute to the dynamic energy release rate.

Keywords: Piezoelectricity; Dynamic response; Singular integral equations; Dynamic stress intensity factor; Dynamic energy release rate

1. Introduction

The wide application of piezoelectric materials in intelligent structural systems makes it necessary to research the fracture problems associated with such defects as cracks and holes. Especially when cracked configurations undergo dynamic loads, whether conventional fracture parameters (e.g., the dynamic stress intensity factor) can be adopted to predict the unstable fracture of piezoelectric materials constitutes an important problem to be solved. Chen and Yu (1997, 1998) investigated the dynamic

* Corresponding author. Fax: +86-10-6278-1824.
E-mail address: yusw@mail.tsinghua.edu.cn (S. Yu).

0020-7683/00/$ - see front matter
PII: S0020-7683(99)00268-1

responses of a finite crack and a semi-infinite crack in a piezoelectric material, respectively. Khutoryansky and Sosa (1995) presented the dynamic fundamental solutions for piezoelectric materials. Li and Mataga (1996a, 1996b) studied the crack propagation by means of Wiener-Hopf and Cagniard-de Hoop techniques. They introduced such electrical boundaries as conducting electrode and vacuum zone to meet Bleustein-Gulyaev wave phenomenon. For scattering of incident waves from the crack, Shindo and Ozava (1990), Shindo et al. (1996) and Narita and Shindo (1998) investigated, respectively, the diffraction of normally incident longitudinal waves by a Griffith crack in an infinite piezoelectric material, the scattering of Love waves by an edge crack in piezoelectric layered media, and the dynamic response of a cracked dielectric medium in a uniform electric field. In this paper, we study the transient response of a center-situated crack in a piezoelectric strip under anti-plane and electrical impacts. How to impose the electrical boundary conditions on the crack surfaces for piezoelectric fracture analysis remains a controversial problem (see, e.g., Pak, 1990; Suo et al., 1992). Here, we consider a crack with the impermeable surface condition as (see, e.g., Pak, 1990; Li et al., 1990)

$$D_{\mathrm{n}}^{+} = D_{\mathrm{n}}^{-} = 0$$

and a crack with the electrical contact surface condition as (see, e.g., Parton, 1976)

$$D_{\mathrm{n}}^{+} = D_{\mathrm{n}}^{-} \quad \phi^{+} = \phi^{-}$$

where D_{n} is the electric displacement in the direction normal to the crack surface, and ϕ denotes the electric potential. Integral transforms and dislocation density functions are used to reduce the problem to singular integral equations that can be solved numerically. For the impermeable crack, the results indicate that the loading combination parameter has a significant effect on the dynamic stress intensity factor and the dynamic energy release rate which depend on the ratio of crack length to strip width as well. The results also show that the crack extension may be retarded by adjusting the loading combination parameter which determines the contribution from electrical fields to the dynamic energy release rate, this is different from the electrical contact case where electrical fields do not contribute to the dynamic energy release rate.

2. Basic equations

Consider a piezoelectric strip of the width $2h$ that contains a center-situated Griffith crack of length $2c$ with reference to the rectangular coordinate system x, y, z, as shown in Fig. 1. The strip exhibits transversely isotropic behavior and is poled in z-direction. The anti-plane shear impact and the electric displacement impact are imposed on the crack surfaces at $t = 0$. In Fig. 1, $H(t)$ denotes the Heaviside unit step function, c_{44}, ρ, e_{15} and ε_{11} stand for the elastic stiffness constant, the mass density, the piezoelectric constant and the dielectric constant, respectively. We consider only the out-of-plane displacement and the in-plane electric field, that is

$$u_x = u_y = 0 \qquad u_z = w(x, y, t) \tag{1}$$

$$E_x = E_x(x, y, t) \qquad E_y = E_y(x, y, t) \quad E_z = 0 \tag{2}$$

where u_x, u_y, u_z and E_x, E_y, E_z are the components of the displacement and electric field vectors. The constitutive relations are as follows

$$\sigma_{xz} = c_{44} w_{,x} + e_{15} \phi_{,x} \tag{3}$$

$$\sigma_{yz} = c_{44} w_{,y} + e_{15} \phi_{,y} \tag{4}$$

$$D_x = e_{15} w_{,x} - \varepsilon_{11} \phi_{,x} \tag{5}$$

$$D_y = e_{15} w_y - \varepsilon_{11} \phi_{,y} \tag{6}$$

$$E_x = -\phi_{,x} \qquad E_y = -\phi_{,y} \tag{7}$$

where σ_{xz}, σ_{yz} and D_x, D_y are the components of the stress tensor and electric displacement vector, respectively, and ϕ denotes the electrical potential. The governing equations are

$$c_{44} \nabla^2 w + e_{15} \nabla^2 \phi = \rho \frac{\partial^2 w}{\partial t^2} \tag{8}$$

$$e_{15} \nabla^2 w - \varepsilon_{11} \nabla^2 \phi = 0 \tag{9}$$

where $\nabla^2 = \partial^2 / \partial x^2 + \partial^2 / \partial y^2$ is the two-dimensional Laplace operator.

The boundary conditions for the impermeable case are

$$\sigma_{yz}(x, 0, t) = -\tau_0 H(t) \quad -c < x < c \tag{10}$$

$$D_y(x, 0, t) = -D_0 H(t) \quad -c < x < c \tag{11}$$

$$w(x, 0, t) = 0 \quad c < |x| < h \tag{12}$$

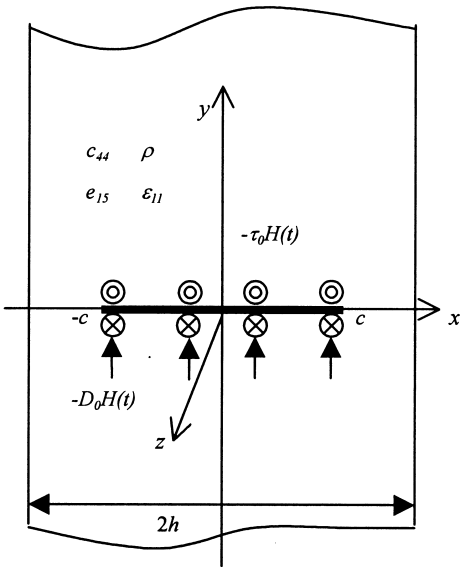

Fig. 1. A piezoelectric strip with a center-situated crack under anti-plane mechanical impact and electrical impact.

$$\phi(x, 0, t) = 0 \quad c < |x| < h \tag{13}$$

$$\sigma_{xz}(\pm h, y, t) = 0 \quad -\infty < y < +\infty \tag{14}$$

$$D_x(\pm h, y, t) = 0 \quad -\infty < y < +\infty \tag{15}$$

For the electrical contact case, the boundary conditions become

$$\sigma_{yz}(x, 0, t) = -\tau_0 H(t) \quad -c < x < c \tag{16}$$

$$w(x, 0, t) = 0 \quad c < |x| < h \tag{17}$$

$$\phi(x, 0, t) = 0 \quad -h < x < h \tag{18}$$

$$\sigma_{xz}(\pm h, y, t) = 0 \quad -\infty < y < +\infty \tag{19}$$

$$D_x(\pm h, y, t) = 0 \quad -\infty < y < +\infty \tag{20}$$

and the electric displacement on the crack surfaces $D_y(x, 0, t)$ consists of two parts, the imposed $-D_0 H(t)$ and the unknown caused by $-\tau_0 H(t)$.

Introducing Laplace transform as follows

$$w^*(x, y, s) = \int_0^{+\infty} w(x, y, t) \exp(-st)\, \mathrm{d}t \tag{21}$$

$$\phi^*(x, y, s) = \int_0^{+\infty} \phi(x, y, t) \exp(-st)\, \mathrm{d}t \tag{22}$$

$$w(x, y, t) = \frac{1}{2\pi i} \int_{Br} w^*(x, y, s) \exp(st)\, \mathrm{d}s \tag{23}$$

$$\phi(x, y, t) = \frac{1}{2\pi i} \int_{Br} \phi^*(x, y, s) \exp(st)\, \mathrm{d}s \tag{24}$$

where Br denotes the Bromwich path.

Noticing that the mechanical–electrical fields are physically antisymmetric with respect to the plane $y = 0$ and symmetric with respect to $x = 0$, Fourier cosine and sine transforms are applied to give the solutions as

$$w^*(x, y, s) = \frac{2}{\pi} \int_0^{+\infty} A_1(\xi, s) \exp(-\alpha y) \cos(\xi x)\, \mathrm{d}\xi + \frac{2}{\pi} \int_0^{+\infty} A_2(\xi, s) \cosh(\alpha x) \sin(\xi y)\, \mathrm{d}\xi \tag{25}$$

$$\phi^*(x, y, s) = \frac{2}{\pi}\int_0^{+\infty}\left[\frac{e_{15}}{\varepsilon_{11}}A_1(\xi, s)\exp(-\alpha y) - \frac{1}{\varepsilon_{11}}B_1(\xi, s)\exp(-\xi y)\right]\cos(\xi x)\,\mathrm{d}\xi + \frac{2}{\pi}\int_0^{+\infty}\left[\frac{e_{15}}{\varepsilon_{11}}A_2(\xi, s)\cosh(\alpha x) - \frac{1}{\varepsilon_{11}}B_2(\xi, s)\cosh(\xi x)\right]\sin(\xi y)\,\mathrm{d}\xi \tag{26}$$

where $A_1(\xi, s)$, $A_2(\xi, s)$, $B_1(\xi, s)$, and $B_2(\xi, s)$ are the unknowns to be solved and

$$\alpha = \sqrt{\xi^2 + \frac{s^2}{c_{\mathrm{T}}^2}} \quad c_{\mathrm{T}} = \sqrt{\frac{(c_{44} + e_{15}^2/\varepsilon_{11})}{\rho}} \tag{27}$$

We proceed with the impermeable case. In Laplace transform domain, substituting Eqs. (25) and (26) into Eqs. (3) and (5), and using Eqs. (14) and (15), we obtain

$$\int_0^{+\infty} A_1(\xi, s)\exp(-\alpha y)\xi\sin(\xi h)\,\mathrm{d}\xi = \int_0^{+\infty}\alpha A_2(\xi, s)\sinh(\alpha h)\sin(\xi y)\,\mathrm{d}\xi \tag{28}$$

$$\int_0^{+\infty} B_1(\xi, s)\exp(-\xi y)\xi\sin(\xi h)\,\mathrm{d}\xi = \int_0^{+\infty} B_2(\xi, s)\xi\sinh(\xi h)\sin(\xi y)\,\mathrm{d}\xi \tag{29}$$

By applying Fourier sine transform (see, e.g., Gradshteyn and Ryzhik, 1980)

$$\exp(-\alpha y) = \frac{2}{\pi}\int_0^{+\infty}\frac{\eta\sin(\eta y)}{\alpha^2 + \eta^2}\,\mathrm{d}\eta \tag{30}$$

From Eqs. (28) and (29), we have

$$\alpha A_2(\xi, s)\sinh(\alpha h) = \frac{2}{\pi}\xi\int_0^{+\infty}\frac{\eta A_1(\eta, s)\sinh(\eta h)}{\alpha^2 + \eta^2}\,\mathrm{d}\eta \tag{31}$$

$$B_2(\xi, s)\sinh(\xi h) = \frac{2}{\pi}\int_0^{+\infty}\frac{\eta B_1(\eta, s)\sinh(\eta h)}{\xi^2 + \eta^2}\,\mathrm{d}\eta \tag{32}$$

Defining dislocation density functions as

$$f(x, s) = \begin{cases}\dfrac{\partial w^*(x, 0, s)}{\partial x} & -c < x < c \\ 0 & c \le |x| \le h\end{cases} \tag{33}$$

$$g(x, s) = \begin{cases}\dfrac{\partial \phi^*(x, 0, s)}{\partial x} & -c < x < c \\ 0 & c \le |x| \le h\end{cases} \tag{34}$$

we obtain

$$A_1(\xi, s) = -\frac{1}{\xi}\int_0^c f(u, s)\sin(\xi u)\,\mathrm{d}u \tag{35}$$

$$B_1(\xi, s) = \frac{1}{\xi}\int_0^c \left[\varepsilon_{11} g(u, s) - e_{15} f(u, s)\right] \sin(\xi u)\, \mathrm{d}u \tag{36}$$

From Eqs. (31) and (32), $A_2(\xi, s)$ and $B_2(\xi, s)$ can be expressed, respectively, as

$$A_2(\xi, s) = -\frac{\xi \exp(-\alpha h)}{\alpha^2 \sinh(\alpha h)} \int_0^c f(u, s) \sinh(\alpha u)\, \mathrm{d}u \tag{37}$$

$$B_2(\xi, s) = -\frac{\exp(-\xi h)}{\xi \sinh(\xi h)} \int_0^c \left[-\varepsilon_{11} g(u, s) + e_{15} f(u, s)\right] \sinh(\xi u)\, \mathrm{d}u \tag{38}$$

3. Singular integral equations and solutions

Substituting Eqs. (25) and (26) into Eqs. (4) and (6) in Laplace transform domain, we obtain

$$\begin{aligned}\sigma^*_{yz}(x, 0, s) = \frac{2}{\pi}\Bigg\{ &-\int_0^{+\infty} \left(c_{44} + \frac{e_{15}^2}{\varepsilon_{11}}\right) \alpha A_1(\xi, s) \cos(\xi x)\, \mathrm{d}\xi + \int_0^{+\infty} \frac{e_{15}}{\varepsilon_{11}} B_1(\xi, s) \xi \cos(\xi x)\, \mathrm{d}\xi \\ &+ \int_0^{+\infty} \left(c_{44} + \frac{e_{15}^2}{\varepsilon_{11}}\right) A_2(\xi, s) \cosh(\alpha x) \xi\, \mathrm{d}\xi - \int_0^{+\infty} \frac{e_{15}}{\varepsilon_{11}} B_2(\xi, s) \cosh(\xi x) \xi\, \mathrm{d}\xi \Bigg\}\end{aligned} \tag{39}$$

$$D^*_y(x, 0, s) = \frac{2}{\pi}\left\{ -\int_0^{+\infty} B_1(\xi, s) \xi \cos(\xi x)\, \mathrm{d}\xi + \int_0^{+\infty} B_2(\xi, s) \xi \cosh(\xi x)\, \mathrm{d}\xi \right\} \tag{40}$$

By means of Eqs. (35)–(38), (10) and (11) in Laplace transform domain, we can obtain following the method developed by Erdogan, 1975 the singular integral equations

$$\begin{aligned}&\frac{c_{44}}{\pi}\int_0^c \frac{f(u, s)}{u - x}\, \mathrm{d}u + \frac{e_{15}}{\pi}\int_0^c \frac{g(u, s)}{u - x}\, \mathrm{d}u + \frac{1}{\pi}\int_0^c \left[Q_{11}(u, x) f(u, s) + Q_{12}(u, x) g(u, s)\right] \mathrm{d}u = -\frac{\tau_0}{s} \\ &\frac{e_{15}}{\pi}\int_0^c \frac{f(u, s)}{u - x}\, \mathrm{d}u - \frac{\varepsilon_{11}}{\pi}\int_0^c \frac{g(u, s)}{u - x}\, \mathrm{d}u + \frac{1}{\pi}\int_0^c \left[Q_{21}(u, x) f(u, s) + Q_{22}(u, x) g(u, s)\right] \mathrm{d}u = -\frac{D_0}{s} \\ &0 < x < c\end{aligned} \tag{41}$$

where $Q_{ij}(\,)$ are, for conciseness, given in Appendix A.

Eq. (41) can be solved by introducing two nondimensional variables ρ and r defined by

$$u = \frac{\rho + 1}{2} c \qquad x = \frac{r + 1}{2} c \tag{42}$$

then Eq. (41) becomes

$$\begin{aligned}
&\frac{c_{44}}{\pi}\int_{-1}^{1}\frac{F(\rho,s)}{\rho-r}\,\mathrm{d}\rho+\frac{e_{15}}{\pi}\int_{-1}^{1}\frac{V(\rho,s)}{\rho-r}\,\mathrm{d}\rho+\frac{1}{\pi}\int_{-1}^{1}\left[\bar{Q}_{11}(\rho,r)F(\rho,s)+\bar{Q}_{12}(\rho,r)V(\rho,s)\right]\mathrm{d}\rho=-\frac{\tau_0}{s}\\
&\frac{e_{15}}{\pi}\int_{-1}^{1}\frac{F(\rho,s)}{\rho-r}\,\mathrm{d}\rho-\frac{\varepsilon_{11}}{\pi}\int_{-1}^{1}\frac{V(\rho,s)}{\rho-r}\,\mathrm{d}\rho+\frac{1}{\pi}\int_{-1}^{1}\left[\bar{Q}_{21}(\rho,r)F(\rho,s)+\bar{Q}_{22}(\rho,r)V(\rho,s)\right]\mathrm{d}\rho=-\frac{D_0}{s}\\
&-1<r<1
\end{aligned}\tag{43}$$

where $F(\,)$, $V(\,)$ and $\bar{Q}_{ij}$ are given in Appendix A.

Based on the numerical method (see, e.g., Erdogan, 1975), $F(\rho,s)$ and $V(\rho,s)$ are expressed as

$$F(\rho,s)=\frac{R(\rho,s)}{\sqrt{1-\rho^2}}\qquad V(\rho,s)=\frac{T(\rho,s)}{\sqrt{1-\rho^2}}\tag{44}$$

and expanding $R(\rho,s)$, $T(\rho,s)$ in forms of Chebyshev polynomials

$$R(\rho,s)=\sum_{i=0}^{\infty}C_iT_i(\rho)\qquad T(\rho,s)=\sum_{i=0}^{\infty}D_iT_i(\rho)\tag{45}$$

It follows that a system of linear algebraic equations can be obtained by using Gauss–Chebyshev formula (see, e.g., Erdogan, 1975)

$$\begin{aligned}
&\sum_{l=1}^{n}\left[\frac{c_{44}}{\rho_l-r_m}+\bar{Q}_{11}(\rho_l,r_m)\right]\frac{R(\rho_l,s)}{n}+\sum_{l=1}^{n}\left[\frac{e_{15}}{\rho_l-r_m}+\bar{Q}_{12}(\rho_l,r_m)\right]\frac{T(\rho_l,s)}{n}=-\frac{\tau_0}{s}\\
&\sum_{l=1}^{n}\left[\frac{e_{15}}{\rho_l-r_m}+\bar{Q}_{21}(\rho_l,r_m)\right]\frac{R(\rho_l,s)}{n}-\sum_{l=1}^{n}\left[\frac{\varepsilon_{11}}{\rho_l-r_m}-\bar{Q}_{22}(\rho_l,r_m)\right]\frac{T(\rho_l,s)}{n}=-\frac{D_0}{s}
\end{aligned}\tag{46}$$

where

$$T_n(\rho_l)=0\quad \rho_l=\cos\left(\frac{2l-1}{2n}\pi\right)\qquad l=1,\ldots n$$

$$U_{n-1}(r_m)=0\quad r_m=\cos\left(\frac{m\pi}{n}\right)\qquad m=1,\ldots n-1$$

We obtain $2(n-1)$ equations with $2n$ unknown quantities to be solved. Noticing that $f(x,s)$, $g(x,s)$ are odd functions with respect to x, i.e., $f(0,s)=0$, $g(0,s)=0$, in other words, $F(\rho,s)$ and $V(\rho,s)$ have no singularities at $\rho=-1$. As in Achenbach et al. (1980) $R(\rho_n,s)$ and $T(\rho_n,s)$ are taken to be zero since ρ_n is the closest of ρ_l to -1 in the limiting sense as $n\to\infty$. Then we can solve this linear algebraic system of $2(n-1)\times 2(n-1)$ to obtain the values of $R(\rho_l,s)$ and $T(\rho_l,s)$.

The dynamic stress intensity factor and the electric displacement intensity factor in Laplace transform domain are determined as

$$K^*_{\mathrm{III}}(c,s)=\lim_{x\to c^+}\sqrt{2(x-c)}\sigma^*_{yz}(x,0,s)\tag{47}$$

$$K^*_{\mathrm{D}}(c,s)=\lim_{x\to c^+}\sqrt{2(x-c)}D^*_{y}(x,0,s)\tag{48}$$

By virtue of the property of Chebyshev polynomials (see, e.g., Erdogan, 1975)

$$\frac{1}{\pi}\int_{-1}^{1}\frac{T_n(u)\,\mathrm{d}u}{(u-x)\sqrt{1-u^2}}=-\frac{|x|}{x\sqrt{x^2-1}}\left[x-\frac{|x|\sqrt{x^2-1}}{x}\right]^n \quad n=0,1,\ldots,|x|>1 \tag{49}$$

we obtain

$$K^*_{\mathrm{III}}(c,s)=-\sqrt{\frac{c}{2}}\left[c_{44}R(1,s)+e_{15}T(1,s)\right] \tag{50}$$

$$K^*_{\mathrm{D}}(c,s)=-\sqrt{\frac{c}{2}}\left[e_{15}R(1,s)-\varepsilon_{11}T(1,s)\right] \tag{51}$$

The Laplace inverse transformations of Eqs. (50) and (51) are carried out by the numerical method developed by Miller and Guy (1966). In this paper, we present the values of $K_{\mathrm{III}}(c,t)$ and $K_{\mathrm{D}}(c,t)$ within a range of $c_{\mathrm{T}}t/c=0$–10.

For the impermeable case, as the electrical impact is loaded, it is not clear that the dynamic stress intensity factor will play the same role as in the purely elastic case. Therefore, we introduce the dynamic energy release rate G as Pak (1990) did.

According to Eqs. (47), (48), (50) and (51), as $x\to c^+$, $\sigma_{yz}(x,0,t)$, $D_y(x,0,t)$ and $w(x,0,t)$, $\phi(x,0,t)$ can be approximated as

$$\begin{Bmatrix}\sigma_{yz}(x,0,t)\\ D_y(x,0,t)\end{Bmatrix}=\frac{1}{\sqrt{2(x-c)}}\begin{Bmatrix}K_{\mathrm{III}}(c,t)\\ K_{\mathrm{D}}(c,t)\end{Bmatrix} \tag{52}$$

$$\begin{Bmatrix}w(x,0,t)\\ \phi(x,0,t)\end{Bmatrix}=\frac{\sqrt{2(c-x)}}{c_{44}\varepsilon_{11}+e_{15}^2}\begin{bmatrix}\varepsilon_{11} & e_{15}\\ e_{15} & -c_{44}\end{bmatrix}\begin{Bmatrix}K_{\mathrm{III}}(c,t)\\ K_{\mathrm{D}}(c,t)\end{Bmatrix} \tag{53}$$

Substituting Eqs. (52) and (53) into

$$Gdc=2\int_c^{c+dc}\frac{1}{2}\left[\sigma_{yz}(x,0,t),D_y(x,0,t)\right]\left[w(x-dc,0,t),\phi(x-dc,0,t)\right]^{\mathrm{T}}\mathrm{d}x \tag{54}$$

yields

$$G=\frac{\pi}{2\left(c_{44}\varepsilon_{11}+e_{15}^2\right)}\left[\varepsilon_{11}K^2_{\mathrm{III}}(c,t)+2e_{15}K_{\mathrm{III}}(c,t)K_{\mathrm{D}}(c,t)-c_{44}K^2_{\mathrm{D}}(c,t)\right] \tag{55}$$

For electrical contact case, the singular integral equation can be derived by a similar method as

$$\frac{c_{44}}{\pi}\int_0^c\frac{f(u,s)}{u-x}\,\mathrm{d}u+\frac{1}{\pi}\int_0^c Q_{11}(u,x)f(u,s)\,\mathrm{d}u=-\frac{\tau_0}{s} \tag{56}$$

and by means of the solutions of Eq. (56), the electric displacement $D^*_y(x,0,s)$ on crack surfaces can be obtained as

$$D^*_y(x,0,s)=\frac{e_{15}}{\pi}\int_0^c\frac{f(u,s)}{u-x}\,\mathrm{d}u+\frac{1}{\pi}\int_0^c Q_{21}(u,x)f(u,s)\,\mathrm{d}u-\frac{D_0}{s} \tag{57}$$

The dynamic stress intensity factor in Laplace domain and the dynamic energy release rate are

$$K^*_{\mathrm{III}}(c, s) = -\sqrt{\frac{c}{2}} c_{44} R(1, s) \tag{58}$$

$$G = \frac{\pi}{2c_{44}} K^2_{\mathrm{III}}(c, t) \tag{59}$$

The analysis of the electrical contact case shows that the imposed electric displacement impact doesn't contribute to the dynamic stress intensity factor and the energy release rate, and the dynamic stress intensity factor remains to be thought of as the fracture parameter as in the purely elastic case. In the absence of the mechanical impact, in other words, the material is in effect seamless as far as the electric field is concerned and the field will not be perturbed by the presence of the crack (see, e.g., McMeeking, 1989).

4. Results and discussion

We carry out numerical calculations for the piezoelectric material $BaTiO_3$ of which the material constants are (see, e.g., Narita and Shindo, 1998)

$$c_{44} = 4.4 \times 10^{10}\ \mathrm{N/m^2} \quad e_{15} = 11.4\ \mathrm{C/m^2}$$

$$\rho = 5700\ \mathrm{kg/m^3} \quad \varepsilon_{11} = 128.3 \times 10^{-10}\ \mathrm{C/Vm}$$

The loading combination parameter λ is determined as $\lambda = D_0 e_{15}/(\tau_0 \varepsilon_{11})$ which is used to reflect the relation between the shear impact $-\tau_0 H(t)$ and the electrical impact $-D_0 H(t)$. Without any loss in generality, we take $\tau_0 = 1.2 \times 10^6\ \mathrm{N/m^2}$, and D_0 is determined by the combination parameter λ. G_0 denotes the energy release rate for the unbounded piezoelectric material subjected to static shear $-\tau_0$, and can be written as (see, e.g., Pak, 1990)

$$G_0 = \pi c \varepsilon_{11} \tau_0^2 / \left(2c_{44}\varepsilon_{11} + 2e_{15}^2\right) \tag{60}$$

In numerical procedure, we take $n = 49$ to insure the precision of 0.00001 for $c/h \leq 0.8$. For the case where only the shear impact is loaded, the results in Fig. 2 indicate that the value of the dynamic stress intensity factor increases quickly with time, reaches a peak value and then decreases oscillating around the corresponding static value. The peak value of the dynamic stress intensity factor will increase as the ratio c/h increases. When the crack tips approach the strip edges, e.g., $c/h = 1/1.25$, the peak value of the dynamic stress intensity factor will become very close to the corresponding static value. This tendency indicates that the boundary effects will dominate the dynamic stress intensity factor for the large value of c/h. The above phenomena can also be observed in Fig. 3. This shows that the dynamic stress intensity factor and the dynamic energy release rate play the same role when only the shear impact is imposed.

Figs. 4–6 show the effects of the loading combination parameter $\lambda = D_0 e_{15}/(\tau_0 \varepsilon_{11})$ on the dynamic stress intensity factor and the dynamic energy release rate for the cases where $c/h = 1/1.5$ and $c/h = 0$. Though the dynamic stress intensity factor will be greater or less than zero in different time domains determined by the sign and magnitude of λ, we cannot dictate that the combination of the external impacts will promote or retard the crack extension. The electrical fields will contribute to the dynamic energy release rate as the impermeable case is considered, so it seems appropriate to introduce the dynamic energy release rate to indicate the crack extension force. Noticing that at $t = 0$, the dynamic

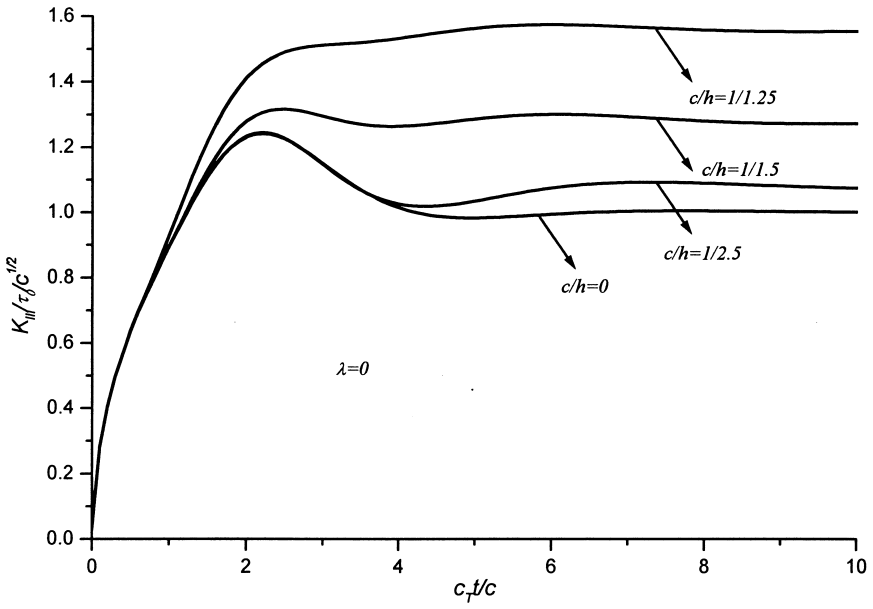

Fig. 2. Normalized dynamic stress intensity factors for various ratios of crack length to strip width with normalized time.

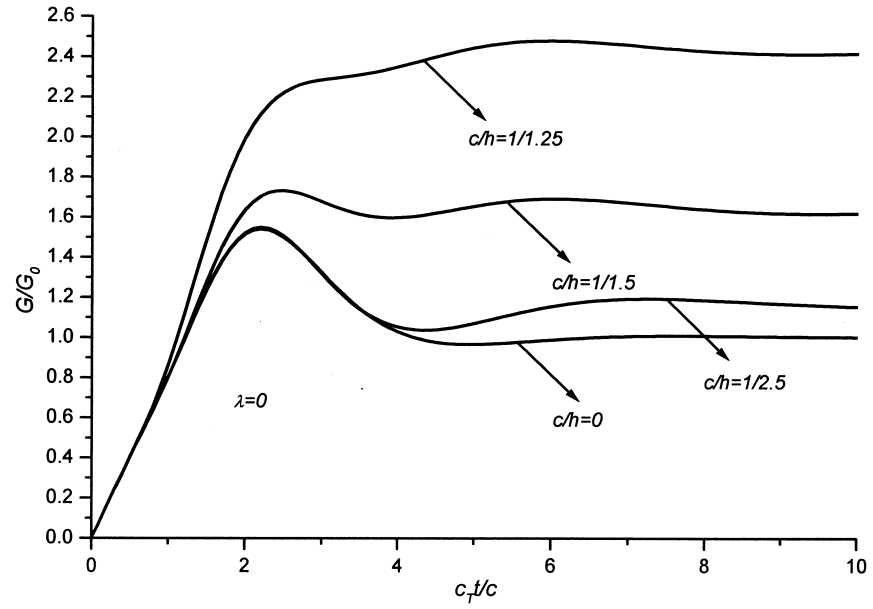

Fig. 3. Normalized dynamic energy release rates for various ratios of crack length to strip width with normalized time.

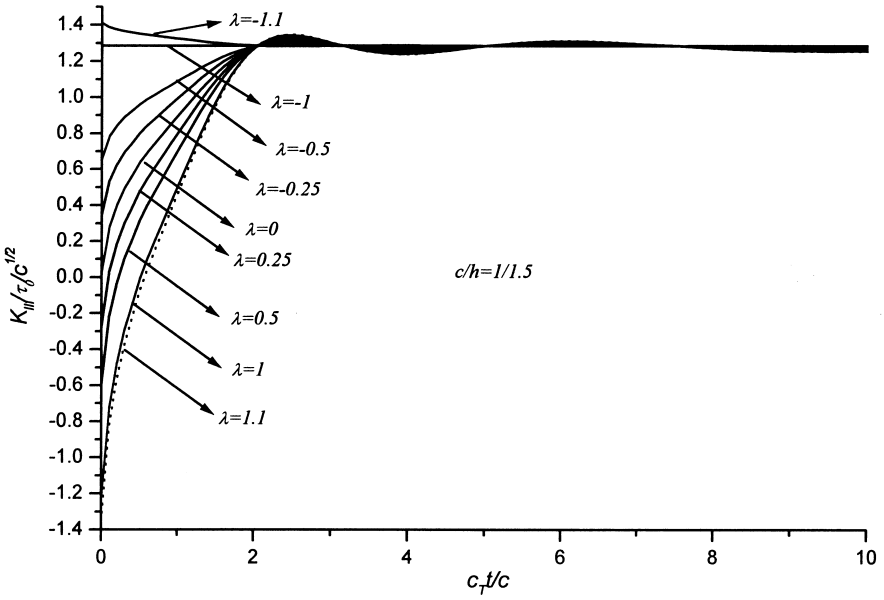

Fig. 4. Normalized dynamic stress intensity factors for various load combination parameters with normalized time.

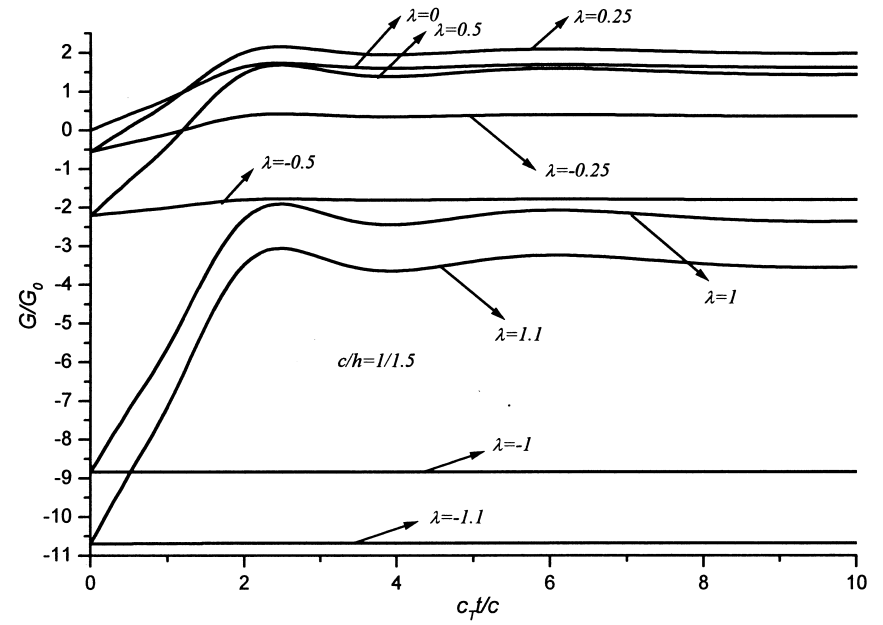

Fig. 5. Normalized dynamic energy release rates for various load combination parameters with normalized time.

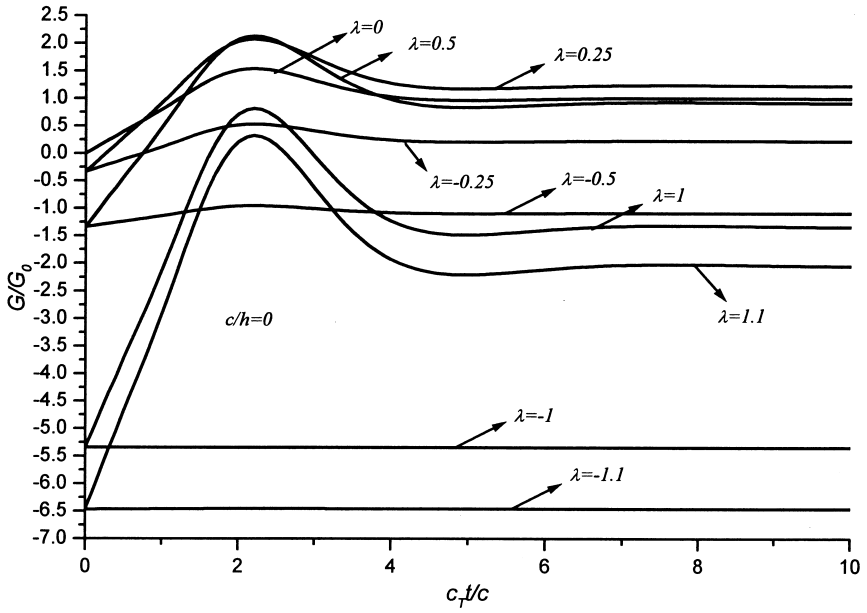

Fig. 6. Normalized dynamic energy release rates stress for various load combination parameters with normalized time.

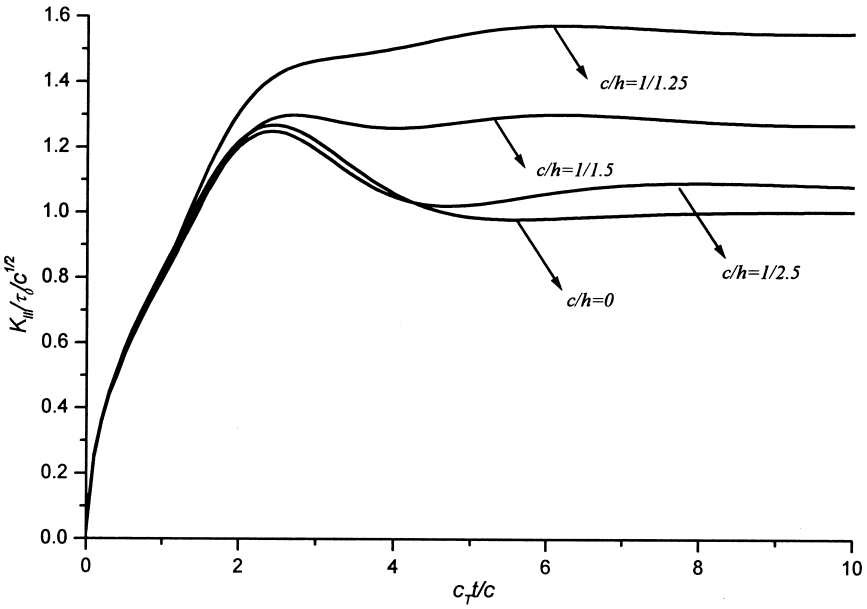

Fig. 7. Normalized dynamic stress intensity factors for various ratios of crack length to strip width with normalized time.

energy release rate for a fixed λ equals to that for $-\lambda$. We take two opposite values of λ as a λ-pair, e.g., $\lambda = 0.5$ and $\lambda = -0.5$ constitute a λ-pair. On the one hand, the results in Figs. 5 and 6 indicate that, as a λ-pair is concerned, the negative electrical impacts imposed on crack surfaces are more liable to promote the crack extension. On the other hand, Figs. 5 and 6 show that the peak value of the dynamic energy release rate depends greatly on the values of λ and c/h. In particular, the value of λ exerts a significant influence on the peak value. In this sense, it can be expected that the crack extension may be retarded by adjusting the loading combination parameter λ.

For the electrical contact case, the crack responses only to the mechanical impact. In Fig. 7, we give the dynamic stress intensity factor as a function of c/h and $c_T t/c$. By comparing the results in Fig. 7 with those in Fig. 2, no distinct difference between them can be found. In the absence of the electrical impact, in other words, the dynamic stress intensity factor is insensitive to the types of electrical boundaries, e.g., the impermeable crack and the electrical contact crack. The results reveal the same interaction between the inertia and the crack geometry characterized by c/h (Fig. 2), and it is this interaction that determines the dynamic stress intensity factor.

Acknowledgements

This project was supported by the National Natural Science Foundation of China under the contract 19891180 and the Post-Doctor's Scientific Foundation of China.

Appendix A

$$Q_{11}(u,x) = \int_0^{+\infty} 2\left(c_{44} + \frac{e_{15}^2}{\varepsilon_{11}}\right)\left(\frac{\alpha}{\xi} - 1\right)\cos(\xi x)\sin(\xi u)\,\mathrm{d}u + \frac{c_{44}}{u+x} - \int_0^{\infty} 2\left(c_{44} + \frac{e_{15}^2}{\varepsilon_{11}}\right)\frac{\xi^2 \sinh(\alpha u)\cosh(\alpha x)}{\alpha^2 \sinh(\alpha h)\exp(\alpha h)}\,\mathrm{d}\xi + \int_0^{+\infty} \frac{2e_{15}^2}{\varepsilon_{11}}\frac{\sinh(\xi u)\cosh(\xi x)}{\sinh(\xi h)\exp(\xi h)}\,\mathrm{d}\xi \tag{A1}$$

$$Q_{12}(u,x) = \frac{e_{15}}{u+x} - \int_0^{\infty} \frac{2e_{15}\sinh(\xi u)\cosh(\xi x)}{\sinh(\xi h)\exp(\xi h)}\,\mathrm{d}\xi \tag{A2}$$

$$Q_{21}(u,x) = Q_{12} \tag{A3}$$

$$Q_{22}(u,x) = -\frac{\varepsilon_{11}}{u+x} + \int_0^{\infty} \frac{2\varepsilon_{11}\sinh(\xi u)\cosh(\xi x)}{\sinh(\xi h)\exp(\xi h)}\,\mathrm{d}\xi \tag{A4}$$

$$F(\rho,s) = f\left(\frac{\rho+1}{2}c, s\right) \qquad V(\rho,s) = g\left(\frac{\rho+1}{2}c, s\right) \tag{A5}$$

$$\bar{Q}_{11}(\rho,r) = \frac{c}{2}Q_{11}\left(\frac{\rho+1}{2}c, \frac{r+1}{2}c\right) \qquad \bar{Q}_{12}(\rho,r) = \frac{c}{2}Q_{12}\left(\frac{\rho+1}{2}c, \frac{r+1}{2}c\right) \tag{A6}$$

$$\bar{Q}_{21}(\rho, r) = \frac{c}{2} Q_{21}\left(\frac{\rho+1}{2}c, \frac{r+1}{2}c\right) \qquad \bar{Q}_{22}(\rho, r) = \frac{c}{2} Q_{22}\left(\frac{\rho+1}{2}c, \frac{r+1}{2}c\right) \tag{A7}$$

References

Achenbach, J., Keer, L., Mendelsohn, D., 1980. Elastodynamic analysis of an edge crack. Journal of Applied Mechanics 47, 551–556.

Chen, Z., Yu, S., 1997. Crack tip fields of piezoelectric materials under anti-plane impact. Chinese Science Bulletin 42, 1615–1619.

Chen, Z., Yu, S., 1998. A semi-infinite crack under anti-plane mechanical impact in piezoelectric materials. International Journal of Fracture 88, L53–L56.

Erdogan, F., 1975. Complex function technique. In: Continuum Physics, vol II. Academic Press, New York, pp. 523–603.

Gradshteyn, I., Ryzhik, I., 1980. Table of Integral, Series and Products. Academic Press, New York.

Khutoryansky, N., Sosa, H., 1995. Dynamic representation formulas and fundamental solutions for piezoelectricity. International Journal of Solids and Structures 32, 3307–3325.

Li, S., Mataga, P., 1996a. Dynamic crack propagation in piezoelectric materials. Part I: Electrode solution. Journal of The Mechanics and Physics of Solids 44, 1799–1830.

Li, S., Mataga, P., 1996b. Dynamic crack propagation in piezoelectric materials. Part II: Vacuum solution. Journal of The Mechanics and Physics of Solids 44, 1831–1866.

Li, S., Cao, W., Cross, L., 1990. Stress and electric displacement distribution near Griffith's type III crack tips in piezoceramics. Material Letters 10, 219–222.

McMeeking, R., 1989. On mechanical stress at cracks in dielectrics with application to dielectric breakdown. Journal of Applied Physics 62, 3116–3122.

Miller, M., Guy, W., 1966. Numerical inversion of the Laplace transform by use of Jacobi polynomials. SIAM Journal Numerical Analysis 3, 624–635.

Pak, Y., 1990. Crack extension force in a piezoelectric materials. Journal of Applied Mechanics 57, 647–653.

Parton, V., 1976. Fracture mechanics of piezoelectric materials. Acta Astronautica 3, 671–683.

Shindo, Y., Ozava, E., 1990. Dynamic analysis of a cracked piezoelectric material. Mechanical Modeling of New Electromagnetic Materials, 297–304.

Shindo, Y., Katsura, H., Yan, W., 1996. Dynamic stress intensity factor of a cracked electric medium in a uniform electric field. Acta Mechanica 117, 1–10.

Narita, F., Shindo, Y., 1998. Scattering of Love waves by a surface-breaking crack in piezoelectric layered medium. JSME International Journal 41, 40–48.

Suo, Z., Kuo, C., Barnett, D., Willis, J., 1992. Fracture mechanics for piezoelectric ceramics. Journal of The Mechanics and Physics of Solids 40, 739–765.